Isospin asymmetries in pion scattering to isoscalar giant quadrupole states in Ni isotopes

D. S. Oakley, M. R. Braunstein, J. J. Kraushaar, R. A. Loveman,
R. J. Peterson, and D. J. Rilett
University of Colorado, Boulder, Colorado 80309

R. L. Boudrie
Los Alamos National Laboratory, Los Alamos, New Mexico 87545
(Received 27 February 1989)

Inelastic scattering of 180 MeV π^- and π^+ from ^{58,60,62,64}Ni shows a prominent quadrupole feature near $65A^{-1/3}$ MeV, identified as the familiar isoscalar giant quadrupole resonance. For the heavier two isotopes, the π^- scattering cross sections greatly exceed those for π^+, the same effect previously noted in pion scattering on heavy nuclei. Since these four nickel targets contain a range of single-nucleon binding energies, these new data demonstrate the influence of these single-particle effects on the apparent isospin response, increasingly neutronlike for the heavier isotopes.

I. INTRODUCTION

If a bulk collective mode of nuclear motion is examined over a range of complex nuclei, the properties of excitation, including the isospin composition, should evolve smoothly. The isoscalar giant quadrupole resonance (GQR) has been observed with an energy centroid of $65A^{-1/3}$ MeV over many targets, with an isoscalar matrix element observed by inelastic alpha scattering to be near 100% of the general energy-weighted sum rule expectation.[1] An explicit study of the isospin nature of the response of this mode is made possible by comparing π^- and π^+ inelastic scattering, with the general result being an excess of π^- over the π^+ cross section, seeming to increase smoothly with target mass.[2] For ^{208}Pb this excess is by a factor near 2.5 and the nuclear matrix elements extracted from these data show a neutronlike amplitude not exhibiting the expected isoscalar symmetry.[3]

This surprising result has brought forth a renewed discussion as to the meaning of the GQR response.[4,5] Recent measurements using neutrons and protons as scattering probes have shown that the GQR in ^{208}Pb appears to be symmetric, and it has therefore been suggested that the interpretation of the pion results is suspect.[6] It is clear, however, that if the sum-rule strength is not of isoscalar symmetry then several important theoretical results would not be vindicated.

The problem is not readily attributed to the reaction mechanism for pions. For low-lying collective excitations, excellent agreement is found comparing pion and electromagnetic studies,[7,8] and such states have been analyzed in the same spectra as the GQR.[2]

Strongly absorbed projectiles such as pions and alphas are particularly sensitive to large nuclear radii, and even a dominantly isoscalar nuclear transition density may not be symmetric between neutrons and protons at these radii. Examples are seen in several random-phase approximation (RPA) calculations,[9,10] and this effect might be expected from the differing contributions of the single-nucleon continuum for these unbound states.

In the present work we examine π^- and π^+ inelastic scattering to the GQR for all four doubly even nickel isotopes. The Coulomb barrier is not so dominant as to allow neutron decay only by default, and a wide range of neutron and proton separation energies is provided (Table I). Over this small range of target masses we compare π^- to π^+ excitation, finding a much more extreme dependence upon the target than expected from the usual simple collective model, but, nonetheless, we extract nuclear matrix elements by the standard collective procedure. These are then compared to sum-rule limits, and for the heavier nickel isotopes, show the same neutronlike enhancement so prominent for heavier targets. These new data thus indicate clearly that collective methods cannot be used to analyze inelastic scattering data to the GQR with strongly absorbed projectiles, and that erroneous conclusions will be, and have been, drawn from such a practice.

II. THE EXPERIMENT

Inelastic pion-scattering spectra were obtained with the EPICS system at the Clinton P. Anderson Meson Physics Facility at Los Alamos National Laboratory, with a beam energy of 180 MeV. Background due to muons was reduced by a range-absorber system, and at small angles an electronic gate was operated to reduce the large elastic scattering peak. Four isotopically enriched targets ($\sim$99% pure ^{58}Ni, ^{60}Ni, ^{62}Ni, and ^{64}Ni), were placed simultaneously in the pion beam spot, with trajectories traced from the origin of each scattered event for sorting into separate histograms. The spectrometer acceptance was centered at 16 MeV of excitation, giving good efficiency from 0 to 30 MeV of excitation. A focal-plane scan determined the solid angle acceptance of the system for each target and comparison to elastic scatter-

TABLE I. Comparison of the GQR systematic excitation energy to neutron and proton separation energies (SE) for the stable doubly even Ni isotopes.

A	$65A^{-1/3}$ (MeV)	SE_n (MeV)	SE_p (MeV)
^{58}Ni	16.79	12.2	8.18
^{60}Ni	16.60	11.4	9.53
^{62}Ni	16.42	10.6	11.1
^{64}Ni	16.25	9.66	12.5

ing from hydrogen in a CH_2 target determined the absolute cross sections. This was checked by comparing the observed Ni elastic scattering cross sections to optical-model predictions, with good agreement. Our absolute cross sections are accurate to within ±8%, but cross sections from target-to-target or angle-to-angle have a systematic uncertainty of ±5%.

Yields for the states in these spectra were obtained by fitting the peaks with Gaussian peak shapes (Lorentzian shapes were also used for comparison), where the resolution of the low-lying states was found to be around 200 keV. Because the giant dipole resonance (GDR) state is unresolved from the GQR in these nickel isotopes, we shall rely on the shapes of the angular distributions to separate the GQR and GDR responses. A range of widths for the GQR peak was used in the fitting procedure at each angle to establish uncertainties in the extracted quantities. Extremes for these yields can also be determined by setting the background to zero and to a constant height at an excitation energy above the GQR. Figure 1 shows a sample spectrum fit using three types of backgrounds, where the giant resonance region can clearly be seen near 16 MeV.

The resulting differential cross sections for this giant resonance peak, at 27°, where the GQR is at a maximum while the GDR is expected to be at a minimum, are listed for the four targets and both beam species in Table II, with the uncertainties shown being from both statistical and peak-width fitting errors. As can be seen in the figure, fits were also made to other higher-lying features seen in the spectra but results were not considered reliable and no cross sections for these states will be shown.

III. REACTION MODELS

Inelastic scattering cross sections were computed in the distorted-wave impulse approximation (DWIA) using the code DWPI.[11] Ground-state neutron and proton distributions to generate the distortions were taken to be equal, with the Woods-Saxon parameters (c, a and w) obtained by elastic electron scattering,[12] with the rms proton radii unfolded from the diffuseness. No second-order terms in the potential were included, but a 28-MeV energy shift[13] was incorporated for the evaluation of the free π-nucleon amplitudes. Tassie transition densities were used to induce the inelastic scattering (except for $L=0$ calculations, where a breathing mode was used[14]), as in our previous GQR pion-scattering studies,[2] using the same neutron and proton distributions.

Separate deformations for the neutron and proton distributions were varied to fit simultaneously the π^- and π^+ differential cross sections. Because the GDR could

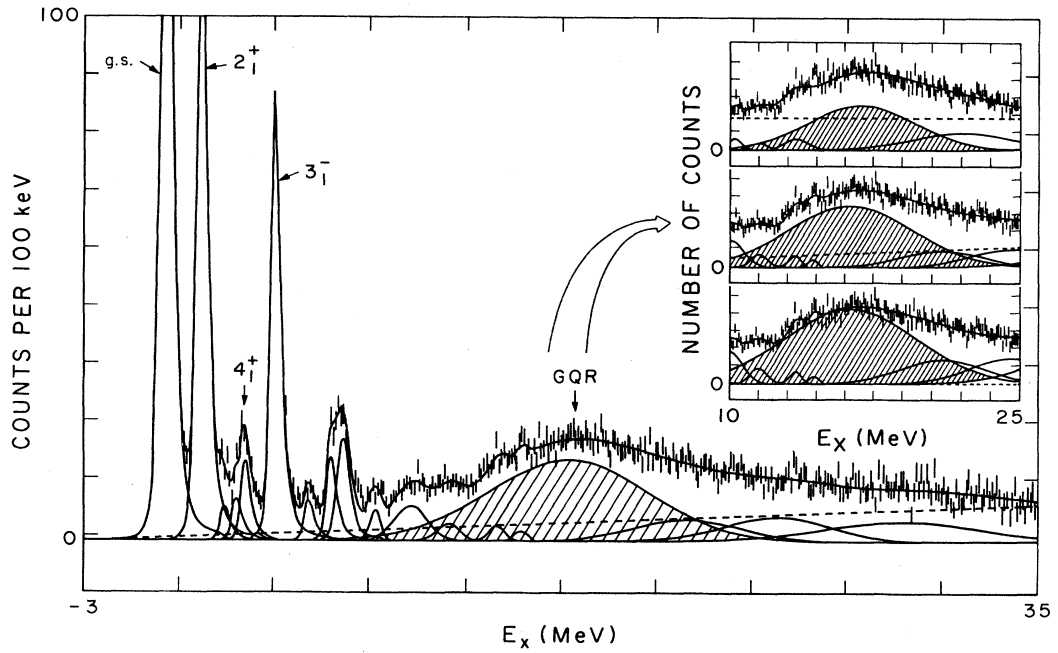

FIG. 1. A sample ^{58}Ni $(\pi^-,\pi^{-'})$ ^{58}Ni spectrum for $T_\pi=180$ MeV at 27° (lab). Here the peaks are fit with Gaussian shapes and a reasonably sloping background (dashed line) labeled "standard" in Table IV. The inset shows this GQR region fitted with the largest reasonable background (top), the standard fit (middle), and a fit with no background (bottom).

TABLE II. GQR cross sections at 27° (corresponding to a minimum for the GDR) and interpolated maximum cross sections. Values taken from "standard" fitting procedure.

A	π^- cross section (mb/sr)	Interpolated (mb/sr)	π^+ cross section (mb/sr)	Interpolated (mb/sr)	Interpolated π^-/π^+
^{58}Ni	6.14(1.07)	8.45	5.28(0.87)	6.35	1.33(.25)
^{60}Ni	4.68(0.96)	6.78	5.02(1.00)	5.99	1.13(.25)
^{62}Ni	10.9(1.09)	16.6	7.13(1.17)	9.01	1.84(.27)
^{64}Ni	8.08(1.18)	13.5	5.01(0.71)	6.48	2.08(.29)

not be resolved from the GQR of interest, this fitting was carried out for the 27° data points, where the GDR yield is a minimum. Results of this fitting are reported as nuclear matrix elements for neutron and proton excitations,

$$M_\mu = \frac{\mu}{4\pi}\int \rho_{tr}(r) r^{L+2} dr \ ,$$

equal in the Tassie model for μ=neutron or proton number to

$$M_\mu = \mu \frac{2L+1}{4\pi} (\beta R)_\mu \langle r^{2L-2}\rangle_\mu / c^{L-1} \ .$$

The moments are evaluated with the ground-state parameters given while the deformation lengths $(\beta R)_\mu$ and relations among them are described in Ref. 2. In a uniform hydrodynamic collective oscillation of the nucleus the ratio of neutron-to-proton matrix elements is given by the ratio

$$M_n/M_p = N/Z \quad \text{(hydrodynamic)} \ .$$

These matrix elements square to give reduced transition probabilities, $B(C2)\uparrow = e^2|M_p|^2$ and $B(N2)\uparrow = |M_n|^2$, and the former may be compared to explicit electromagnetic excitations by electron scattering.

From neutron and proton matrix elements we can also form isoscalar and isovector nuclear matrix elements by

$$M_0 = M_n + M_p$$

and

$$M_1 = M_n - M_p \ ,$$

and thereby the appropriate reduced transition probabilities.

It is useful to compare transition strengths of order L for giant excitations to general sum rules. The appropriate energy-weighted proton quadrupole sum-rule strengths to the isoscalar resonance are given by

$$S_p = \sum \hbar\omega B(C2)\uparrow = \frac{Z^2}{A}\frac{\hbar^2}{2m}\frac{e^2}{4\pi} L(2L+1)^2 \langle r^{2L-2}\rangle_p \ ,$$

using the proton ground-state moment. Other sums to an isoscalar mode are

$$S_n = NS_p/Z$$

and

$$S_0 = A^2 S_p / Z^2 \ .$$

This S_0 is the "classical" isoscalar sum rule of Bohr and Mottelson.[15]

An "isoscalar" oscillation in a nucleus with neutron excess also allows an isovector excitation. For the isovector case we have

$$S_1 = (N-Z)^2 S_0 / A^2 \ .$$

If a single state at $\hbar\omega$=16.4 MeV were to exhaust these sum rules, a scale for the reduced transition probabilities is established. We also quote our results using those sums in terms of the sum-rule fraction (SRF), such as

$$\text{SRF}_p = \hbar\omega M_p^2 / S_p \ .$$

IV. RESULTS AND DISCUSSION

Clear broad peaks are seen at the excitation energy expected for the GQR, as shown in the sample 27° fitted spectra in Fig. 1, which is an angle where the L=1 giant dipole peak is expected to have a minimum cross section. Other important features fit include (for all targets) the low-energy octupole resonance (LEOR),[16] seen near E_x=8 MeV, and the "nose" on the GQR,[17] seen near 13 MeV. Both of these states seem to have flat and possibly octupole (peaking near 30°) shaped angular distributions but are not convincing enough to warrant further discussion, as is the case with three higher-lying resonances seen on all targets to be at around 20, 25, and 30 MeV of excitation, which also seem to peak around 30° but have unreliable shapes. A weak isoscalar giant monopole resonance has been recently observed for ^{58}Ni at an excitation energy of 17.3 MeV.[18] Because this resonance only exhausts 23% of the energy-weighted sum rule (EWSR) we are unable to identify it here, which is a result consistent with previous studies.[19]

The widths of the GQR states were determined from fits to the 27° spectra and found to be 6.8±1 MeV, with a centroid of 16.4±1 MeV for all targets. These excitations are consistent with those reported from electron, proton, and alpha scattering while our widths are greater by 1–2 MeV.[16–26] This greater width can be attributed to uncertainties due to broad features other than the GQR, and this precluded an examination of the greater width anticipated for ^{64}Ni by comparison to a systematic dependence on the GQR excitation energy.[27] The resulting GQR angular distributions are shown for the four targets and both beam species in Figs. 2 and 3.

The solid curves in these figures show the results of the quadrupole fits to our data, demonstrating that the GQR dominates the peak we fit. In order to evaluate the contribution of the GDR we have used the DWIA and the Tassie model, equivalent to a Goldhaber-Teller dipole oscillation, exhausting the classical dipole sum rule.[28] These computed cross sections are shown by the dotted curves, indicating only a small dipole contribution. The figure presenting the ^{58}Ni results also shows the predicted monopole contribution with 23% of the sum rule exhausted (chain-dashed lines in Fig. 2), and this can be seen to be very small. The sums of the dotted and solid curves are shown by the dashed curves. Uncertainties in the GDR and giant-monopole resonance (GMR) yields have negligible impact on our pion GQR results. Uncertainties in GQR matrix elements or reduced transition probabilities include the uncertainty shown for the 27° data points to which we fit.

Pion charge exchange to analogs of the GDR has been observed in ^{60}Ni, with peak differential cross sections less than shown in Fig. 2.[29] When scaled by A, not N or Z, peak pion-scattering cross sections near 1.1 mb/sr are expected, still below the dotted curves. The dashed sum curves in Fig. 2 lie slightly above the small-angle data points, also indicating a smaller GDR cross section than predicted by our calculation.

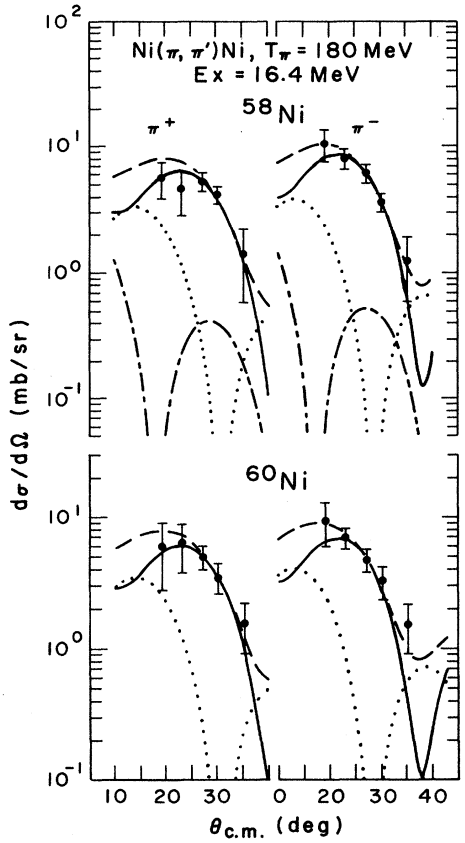

FIG. 2. The GQR angular distributions measured here from ^{58,60}Ni $(\pi,\pi')^{58,60}$Ni at $T_\pi = 180$ MeV ("standard" fit). The solid lines represent the $L=2$ DWIA Tassie model calculation fitted to the data as described in the text, the dotted lines represent the $L=1$ calculation at 100% EWSR, and the dashed lines are the sums. For ^{58}Ni we have included a monopole calculation at 23% EWSR which is shown by the chain-dashed lines.

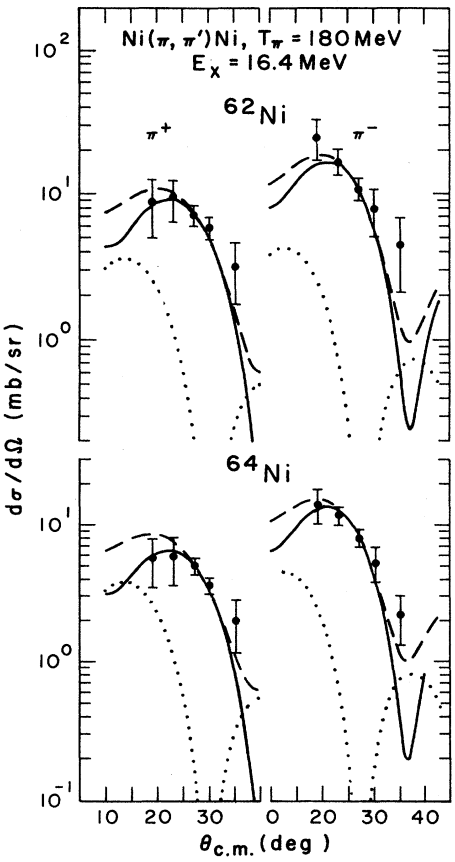

FIG. 3. The GQR angular distributions measured here from ^{62,64}Ni $(\pi,\pi')^{62,64}$Ni at $T_\pi = 180$ MeV ("standard" fit). The solid lines represent the $L=2$ DWIA Tassie model calculation fitted to the data as described in the text, the dotted lines represent the $L=1$ calculation at 100% EWSR, and the dashed lines are the sums.

In Table III our observed ratios of matrix elements M_n and M_p indicate a hydrodynamic GQR response for ^{58}Ni and ^{60}Ni, but not for ^{62}Ni and ^{64}Ni (as also indicated by the cross-section ratios of Table II). For all isotopes measured here, the proton strength remains reasonably con-

TABLE III. Matrix elements extracted for the GQR excitation from the present data by use of the Tassie collective model and the "standard" fitting procedure.

Nucleus	M_p (fm^2)	M_n (fm^2)	M_n/M_n	N/Z
^{58}Ni	33(2)	39(4)	1.18(0.12)	1.07
^{60}Ni	34(3)	36(4)	1.06(0.15)	1.14
^{62}Ni	35(3)	65(4)	1.86(0.20)	1.21
^{64}Ni	28(2)	63(4)	2.25(0.22)	1.29

TABLE IV. A demonstration of the background and fit dependence of the matrix element ratios for the GQR of the Ni isotopes from this work (see Fig. 1). All peak shapes are Gaussians unless otherwise noted.

Nucleus	Model fit	$M_p(e,e')$[a] (fm^2)	$M_p(\pi,\pi')$ (fm^2)	M_n/M_p
^{58}Ni	Standard backgrounds	25(5)	33(2)	1.18(.12)
^{58}Ni	Lorentzian shapes	25(5)	40(4)	1.18(.16)
^{58}Ni	Zero backgrounds	25(5)	35(3)	1.29(.15)
^{58}Ni	Maximum backgrounds	25(5)	26(2)	1.19(.13)
^{64}Ni	Standard backgrounds	<24	28(2)	2.25(.22)
^{64}Ni	Lorentzian shapes	<24	32(2)	2.34(.35)
^{64}Ni	Zero backgrounds	<24	34(4)	2.18(.28)
^{64}Ni	Maximum backgrounds	<24	21(3)	2.26(.33)

[a] ^{58}Ni values from Ref. 21 and ^{64}Ni values from Ref. 26.

stant while the neutrons seem to be primarily responsible for these large, nonhydrodynamic ratios. Our normalizations give elastic angular distributions that are consistent with prediction as well as hydrodynamic ratios for the first 2^+ states for all of the nickel isotopes and so this neutron enhancement in ^{62}Ni and ^{64}Ni is unique to the GQR. It may also be unique to other features in the continuum but a lack of structure combined with the acceptance fall off of the spectra obscures such results.

This GQR neutron enhancement is independent of the background chosen in the fits, as shown by the consistency in the M_n/M_p ratios of Table IV, where we fit the spectra using a variety of background as well as with Lorentzian peak shapes (the resulting angular distributions are similar to the ones in Figs. 2 and 3, except for overall magnitude differences, and so these will not be shown here). We also observe that the reduced transition probabilities extracted from these data are similar to those found from electron- and alpha-scattering measurements (Tables IV and V) if the background dependence is taken into account. For example, our $B(C2)$ value for the GQR in ^{58}Ni is most consistent with the electron-scattering values of Table IV and V if we quote the "maximum-background" results. It can be seen in Table V that many different values of these transition probabilities have been measured for the same GQR states, even when the same probe is used. A comparison of the respective fitting procedures in these different measurements seems to indicate that the above-mentioned background dependence may account for much of this difference. In Table V we quote the value of the "standard" background because we believe this represents the most realistic continuum and quote other backgrounds for demonstration only. As mentioned, this inconsistency in background choice is minimized here for the results that depend on ratios of negative and positive pion cross sections, such as M_n/M_p.

In pion scattering, the π^- predominantly excites the neutron piece of the GQR isoscalar response while the π^+ predominantly excites the protons and so it is infor-

TABLE V. Reduced proton, neutron, and isoscalar transition probabilities (squared matrix elements) for GQR excitations from the present work (first entry) are compared to other results and to the expected energy-weighted sum rules as the percentage.

Nucleus	$B(C2)\uparrow$ (e^2fm^4; SRF)	$B(N2)\uparrow$ (fm^4; SRF)	$B(O2)\uparrow$ (fm^4; SRF)
^{58}Ni	1100; 114(10)% 65(10)%[a] 54(10)%[c]	1500;135(27)%	5200;126(22)% 100(20)%[b] 55(15)%[d] 38(8)%[e]
^{60}Ni	1200; 127(21)% 55(10)%[a]	1300;105(24)%	4900;112(23)% 63(15)%[f]
^{62}Ni	1200;130(22)%	4200;308(37)%	10 000;221(31)%
^{64}Ni	800;85(11)% <60%[g]	4000;259(32)%	8300;170(23)%

[a] Values from (e,e'), Ref. 21.
[b] Values from (α,α'), Ref. 24.
[c] Values from (e,e'), Ref. 27, errors estimated.
[d] Values from (α,α'), Ref. 22.
[e] Values from (α,α'), Ref. 18.
[f] Values from (α,α'), Ref. 23.
[g] Values form (e,e'), Ref. 26.

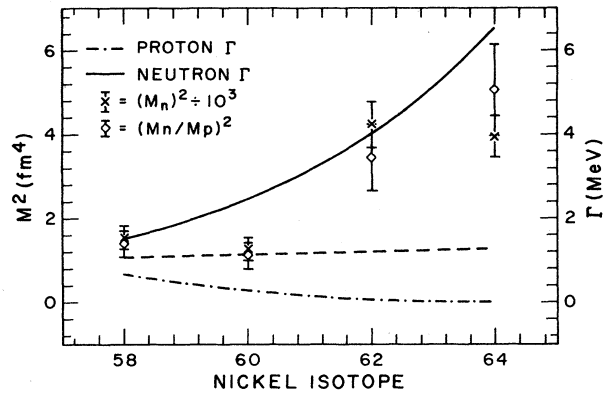

FIG. 4. Matrix elements extracted from these data are compared to the effects of neutron and proton separation energies. Here the separation effects are modeled by single-particle widths (in MeV), as discussed in the text, with the proton width given by the chain-dashed line, the neutron given by the solid line, and the $(N/Z)^2$ prediction by the dashed line.

mative to calculate the single-particle decay widths of this $2\hbar\omega$ response. We have simulated these widths by calculating proton or neutron stripping reactions to the proper GQR quantum numbers using the code DWUCK4.[30] These widths, for neutron and proton decays separately, are shown in Fig. 4, along with the matrix elements from Table III. A $2f_{7/2}$ single-particle state is taken with a decay energy to the lowest $\frac{3}{2}^-$ daughter, where this f-wave state is the average of the $2\hbar\omega$ promotions possible.

Even though there is no formal connection between the excitation of the GQR and the single-particle decays, we see a striking similarity between the neutron excitation probability (M_n, largely from π^-) and the neutron decay strength (Γ_n). The difference between the Γ_n calculations for different isotopes is purely due to the separation energy differences while Coulomb effects tend to make the Γ_p results consistent for all isotopes. This is the result we also see for the excitation of the GQR, an increasing neutron strength while the proton matrix elements remain fairly constant, as seen from the M_n/M_p values extracted from these pion-scattering data.

ACKNOWLEDGMENTS

This work was supported in part by the U.S. Department of Energy. We would like to thank H. Fortune and R. Burman for the use of their nickel targets.

[1]J. Speth and A. van der Woude, Rep. Prog. Phys. **44**, 46 (1981).
[2]J. L. Ullmann *et al.*, Phys. Rev. C **35**, 1099 (1987).
[3]S. J. Seestrom-Morris *et al.*, Phys. Rev. C **33**, 1847 (1986).
[4]D. J. Horen, J. R. Beene, and F. E. Bertrand, Phys. Rev. C **37**, 888 (1988).
[5]V. R. Brown, J. A. Carr, V. A. Madsen, and F. Petrovich, Phys. Rev. C **37**, 1537 (1988).
[6]E. L. Hjort *et al.*, Phys. Rev. Lett. **62**, 870 (1989).
[7]D. S. Oakley and H. T. Fortune, Phys. Rev. C **37**, 1126 (1988).
[8]C. L. Morris *et al.*, Phys. Rev. C **35**, 1388 (1987).
[9]N. Auerbach, A. Klein, and E. R. Siciliano, Phys. Rev. C **31**, 682 (1985).
[10]R. J. Peterson and R. DeHaro, Nucl. Phys. **A459**, 445 (1986).
[11]R. A. Eisenstein and G. A. Miller, Comput. Phys. Commun. **11**, 95 (1976).
[12]H. DeVries, C. W. DeJager, and C. DeVries, At. Data Nucl. Data Tables **36**, 495 (1987).
[13]W. B. Cottingame and D. B. Holtkamp, Phys. Rev. Lett. **45**, 1828 (1980).
[14]G. R. Satchler, Part. Nucl. **5**, 105 (1973).
[15]A. Bohr and B. R. Mottelson, *Nuclear Structure* (Benjamin, Reading, 1975), Vol. II, p. 404.
[16]M. Fujiwara *et al.*, Phys. Rev. C **37**, 2885 (1988).
[17]K. T. Knopfle *et al.*, J. Phys. G **7**, L99 (1981).
[18]G. Duhamel *et al.*, Phys. Rev. C **38**, 2509 (1988).
[19]U. Garg *et al.*, Phys. Rev. C **25**, 3204 (1982).
[20]I. S. Gul'karov, Yad. Fiz. **20**, 17 (1974) [Sov. J. Nucl. Phys. **20**, 9 (1975)].
[21]R. Pitthan *et al.*, Phys. Rev. C **21**, 147 (1980).
[22]D. H. Youngblood *et al.*, Phys. Rev. C **23**, 1997 (1981).
[23]D. H. Youngblood *et al.*, Phys. Rev. C **13**, 994 (1976).
[24]A. Bonin *et al.*, Nucl. Phys. **A430**, 349 (1984).
[25]D. C. Kocher *et al.*, Phys. Rev. Lett. **31**, 1070 (1973).
[26]R. J. Peterson *et al.* (unpublished).
[27]R. A. Loveman and R. J. Peterson, Z. Phys. A **328**, 281 (1987).
[28]B. L. Berman and S. C. Fultz, Rev. Mod. Phys. **47**, 713 (1975).
[29]A. Erell, *et al.*, Phys. Rev. C **34**, 1822 (1986).
[30]P. D. Kunz, code DWUCK4, University of Colorado (unpublished).